DE GRUYTER OPEN

Acta Geophysica
vol. 64, no. 4, Aug. 2016, pp. 943-962
DOI: 10.1515/acgeo-2016-0001

Magnetic and Electromagnetic Signatures around Polile Tshisa Hot Spring in the Northern Neotectonic Belt in the Eastern Cape Province, South Africa

Kakaba MADI[1], Peter K. NYABEZE[2], Oswald GWAVAVA[1], Matome SEKIBA[2], and Baojin ZHAO[3]

[1]Department of Geology, University of Fort Hare, Alice, South Africa
e-mail: kmadi@ufh.ac.za

[2]Geophysics Unit, Council for Geoscience, Pretoria, South Africa

[3]Worley Parsons TWP, Johannesburg, South Africa

A b s t r a c t

Finding productive boreholes in the Karoo fractured aquifers has never been an easy task. Fractured Karoo aquifers in the neotectonic zones in the Eastern Cape Province can be targeted for groundwater exploration. The Polile Tshisa hot spring is located in a seismo-tectonic region beset by neotectonics. Hot springs are indicative of circulation of groundwater at great depths along fault zones, and accordingly of neotectonics. The characterisation of hot springs by means of magnetic and electromagnetic methods can help infer the occurrence of structures which are favourable for groundwater potential. The Polile Tshisa hot spring is characterised by faults, fractures, and dolerite dykes. All these structures make the hot spring a good case study for groundwater exploration.

Key words: neotectonics, electromagnetic, groundwater, hot springs, Karoo.

1. INTRODUCTION

The Eastern Cape northern neotectonic belt is mainly characterized by the Kokstad–Koffiefontein seismic belt (formerly known as the Senqu seismotectonic belt) and seven hot springs (Fig. 1). Meissner and Wever (1986) have shown that epicentres of intracontinental earthquakes (*e.g.*, South Africa) are concentrated on lineaments. Recent seismic activity in the South Africa–Lesotho border region is related either to the southwards propagation of the East Africa Rift System at the boundary between the Nubian and Somalian lithospheric plates, or to epirogenic causes involving a lithospheric Quathlamba hot spot (in the Drakensberg volcanic region), which is a seismicity axis (Hartnady 1985).

Olivier (1972) found that during the construction of the Orange–Fish tunnel, flooding occurred after an abnormally well-developed fissure-zone was intersected approximately 550 m south of the shaft 2. The inrush of water was associated with the collapse of the tunnel roof, as part of the roof's major fissure was exposed by the fateful blast. He noted, however, that an influence of earthquakes and accordingly of neotectonics on the pattern of

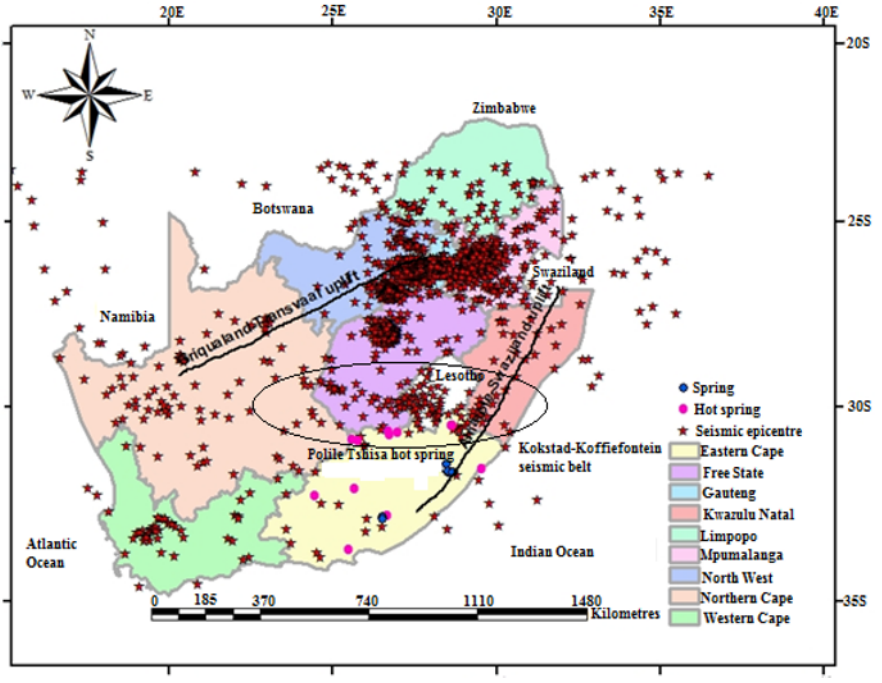

Fig. 1. Seismic epicentres in southern Africa. Note the encircled Kokstad–Koffiefontein seismic belt with its seven hot springs in the Eastern Cape northern neotectonic belt near the country of Lesotho (source of epicentres for new seismic events: IRIS website browser 2012).

semi-diurnal tidal fluctuations is of special interest as regards the flooding problem. Hot springs are indicative of possible neotectonics. It can be suggested that the basaltic eruption of 1983 in Lesotho (Maud *et al.* 1983) might have heated the water from beneath. Moreover, Kent (1969) has shown that the origin of thermal springs is attributed to the presence of deep structures, principally fault-zones, which provide continuously circulating convection or artesian systems. On the other hand, Olivier *et al.* (2011) highlighted that South African thermal springs are some of the most under-researched and under-utilised of all natural resources. Delvaux and Mahon (1993), for instance, compiled a neotectonic map of the Mbeya area in Tanzania from the Quaternary structural elements and volcanic centres, active hot springs, and earthquake epicentres. On the other hand, they highlighted from the works of Spurr (1953) that the hydrothermal activity is rather frequent in the Mbeya area, and is clearly controlled by an active fault. The seven hot springs in the northern neotectonic belt in the Eastern Cape Province are clearly controlled by a neotectonic fault because of the following reasons: the Polile Tshisa hot spring, for instance, is located near the country of Lesotho; the basaltic event of 1983, as reported by Maud *et al.* (1983), is accordingly a neovolcanic event, which has disturbed the crust inducing neotectonics. The Polile Tshisa hot spring is aligned with six other hot springs (on its left) along a neotectonic fault in the Kokstad–Koffiefontein seismic belt (Fig. 1); neotectonics is strongly related to seismic activity.

In a reference guide on geophysical techniques (1993), documented by the Eastern Research Group from Lexington in the United States of America, it was reported that geophysical techniques are used to assess the physical and chemical properties of soils, rocks and groundwater based on response to either (i) various parts of the electromagnetic (EM) spectrum, including gamma rays, visible light, radar, microwave, and radiowaves; (ii) acoustic and/or seismic energy; or (iii) other potential fields such as gravity and the earth's magnetic field. On the other hand, it was shown that the greatest benefits of geophysical methods come from using them early in the site characterization, since they are typically non-destructive, less risky, and require less time and cost than using monitoring wells. Magnetic and electromagnetic surveys can help to characterise potential aquifers as far as the structures are concerned.

2. METHODOLOGY

The northern neotectonic belt of the Eastern Cape Province, due to the remarkable seismic belt that runs from the east coast to Koffienfontein and the presence of many hot springs, is considered as an area of remarkable neotectonics. On the basis of this fact it was suggested that this neotectonic belt could be characterized using geophysics (electromagnetic, magnetic, and

radiometric measurements). Magnetic field data were acquired in the walking mode using a Geometrics Proton Processor Magnetometer (G-859) set to operate in the Julian calendar at a cycle time of 1.5 s, with a resolution of 0.1 nT, and an accuracy of 0.5 nT, at temperatures between –20 and 50°C, and a gradient tolerance of 1000 nT/m. The magnetic maps around the Polile Tshisa hot spring were produced using the Geosoft 7.3 first at a grid cell size of 1 m in order to see all the high frequency signals, then the grid cell size was changed to 14 m so that a generalized complete image can be visualized making it easier to depict a preliminary interpretation.

Electromagnetic measurements are mainly used to depict fissured zones, and were conducted using the Geonics EM ground conductivity meter. The data acquisition was not easy due to accessibility problems. In the area of the hot spring of Polile Tshisa, for instance, houses have been built and big gullies, difficult to cross, were great obstacles. For electromagnetic measurements, a 10-, 20-, and 40-m coil separation cable was used .The conductivity was measured both in horizontal and vertical dipole modes. These measurements were then plotted against the station intervals for each coil separation cable on a binary diagram in order to obtain a profile. At Polile Tshisa the electromagnetic survey was done in the southeast-northeast and southwest-northeast directions (*e.g.*, Fig. 8). These survey lines were set in order to possibly cross cut the fault that host the hot springs. The hydrogeological conceptual model was done using the acquired magnetic data.

3. RESULTS

3.1 Field observations

The Polile hot spring located south of Matatiele near the border of Lesotho is possibly hosted within a major regional fault that connects the hot spring of

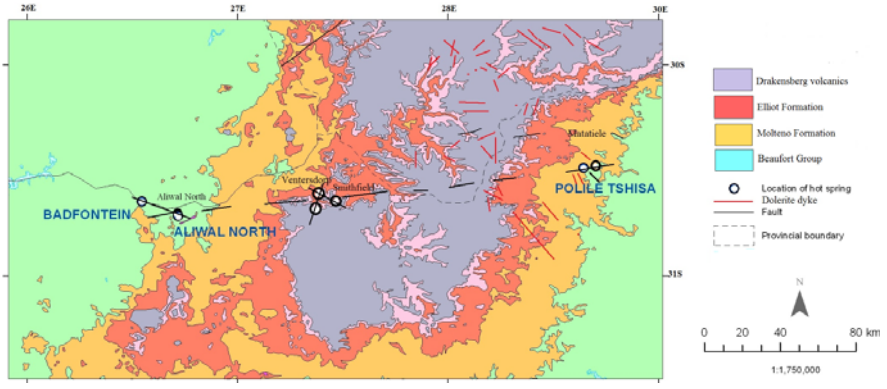

Fig. 2. Geological map showing some structures and the hot springs in the Eastern Cape Province northern neotectonic belt.

Aliwal North and Badfontein (Fig. 2). The water of this hot spring wells up at three different places (Fig. 3a) separated by a distance of almost thirty centimetres aligned in a direction of 75°N. A quartz vein indicating hydrothermal activity occurs near the hot spring. The water of the Polile Tshisa is alkaline (pH of 9.2), and is mainly used by villagers for their domestic

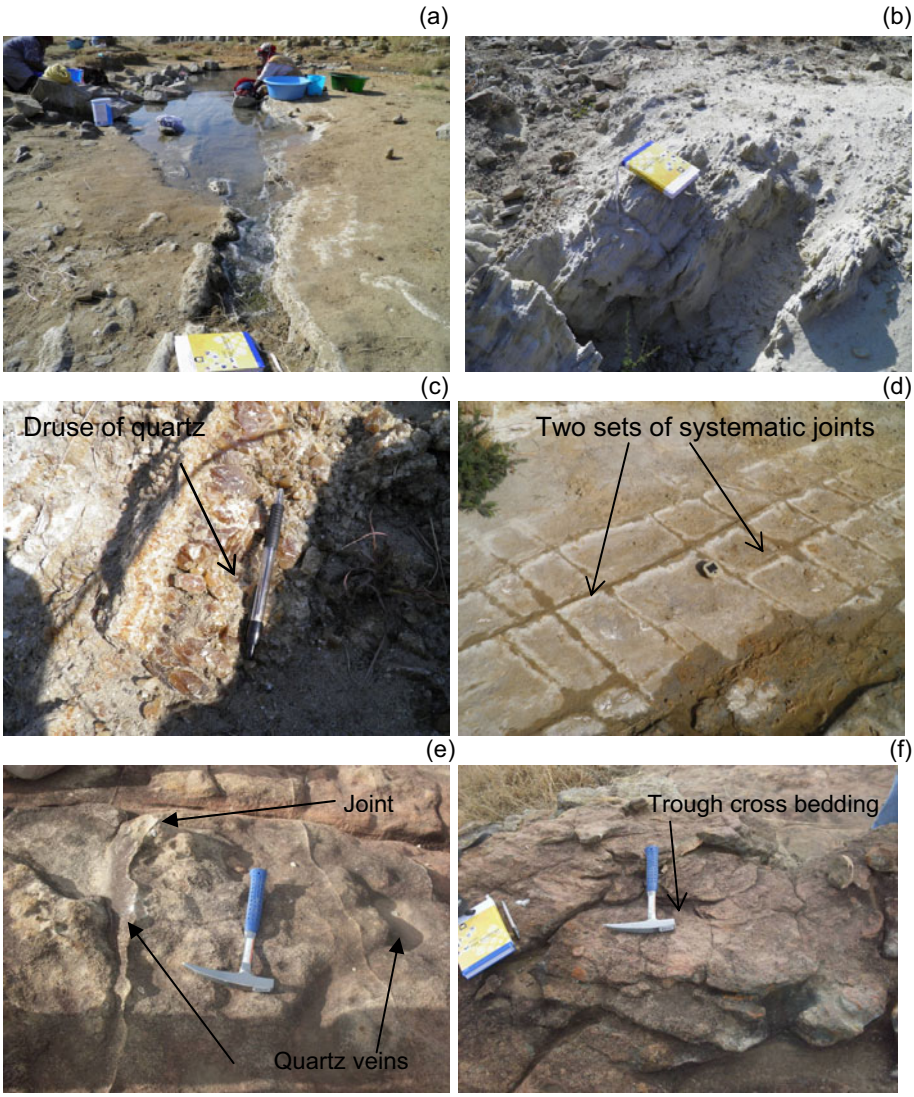

Fig. 3. Caption on next page.

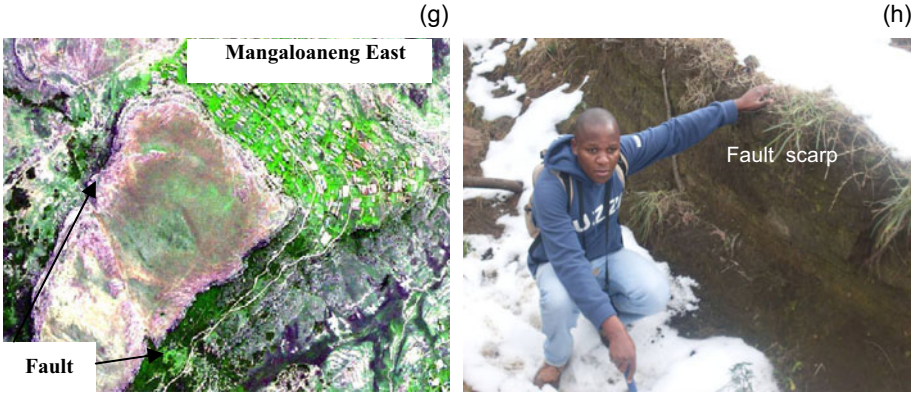

Fig. 3: (a) Polile Tshisa hot spring, (b) intense weathering marked by a kaolinisation, (c) druse of quartz, (d) and (e) centimetric quartz veins, (f) trough-cross bedding, (g) neotectonic fault seen from SPOT data near Mangaloaneng-East village, and (h) fault scarp of the neotectonic fault seen in panel (g).

needs. The temperature of this hot spring water can reach 32°C. The flow rate is of a tiny seep, the water from this hot springs flows along a stream connected to a river nearby. The area itself has outcrops of coarse grains sandstones of the Molteno Formation in the Karoo Supergroup. It is characterized by intense weathering marked by a kaolinisation (Fig. 3b). This weathering indicates an intensive surface water circulation, which is a major source of recharge. The water possibly goes deep down below, and is discharged through the springs. The high degree of weathering has made some of the original rock to completely alter. The sandstone layers have a thickness that varies from 2 to 5 cm. A druse of quartz full of impurities colouring them in brown was seen near the spring (Fig. 3c) and because of weathering, crystals of quartz are easily being loosed up. Two sets of centimetric quartz veins cross cutting each *e* (Fig. 3d) were found on the bed of a non-perennial river near the hot spring; the first set, which is the old one, if the cross cutting relation is applied, has a strike of 320°N; and the second set which is the later one, has a strike of 245°N. The two sets are almost perpendicular, they occur in weathered sandstones with few intercalations of weathered shales. At this place, the beds strike is 250°N, the dip is 15° and the dip direction is 340°N. Similar quartz veins have been found within some coarse-grained sandstones (with a diameter varying between 2 and 5 mm) 10 km north of the Polile Tshisa hot spring near the town of Matatiele around the South Africa–Lesotho border (Fig. 3e). Trough-cross beddings were the only predominant sedimentary structures seen within these sandstones (Fig. 3f). In this area a fault oriented 120°N was depicted from SPOT data around the Mangaloaneng–East village near Matatiele (Fig. 2g); its scarp is visible in

Fig. 3h. This fault indicates neotectonic movement in the area because it has also affected the soil, as can be seen in Fig. 3g.

3.2 Magneitc survey at Polile Tshisa hot spring

The magnetic survey (see sample in Table 1) was conducted around the Polile Tshisa hot spring. This survey was complicated by uneasy accessibility marked by the presence of gullies and some few constructions in the vicinity. Data acquisition was carried out using a Cesium vapour high precision magnetometer (Geometrics 859) along four lines (NW-SE, N-S, NE-SW); these lines can be seen in Fig. 4. Figure 5 shows the grid size expanded to 14 m for a better visualisation. The N-S magnetic line at the right hand side has magnetic high values in the southern area. This might be related to the occurrence of a dolerite dyke, which is a good indicator for drilling in order to generate a potential high yield well.

Three magnetic profiles were extracted from the map in Fig. 5. The first line, SE-NW, has a profile that is almost flat at the right side (Fig. 6). It shows an increase from 10 m reaching more than 27634.4 nT at approxi-

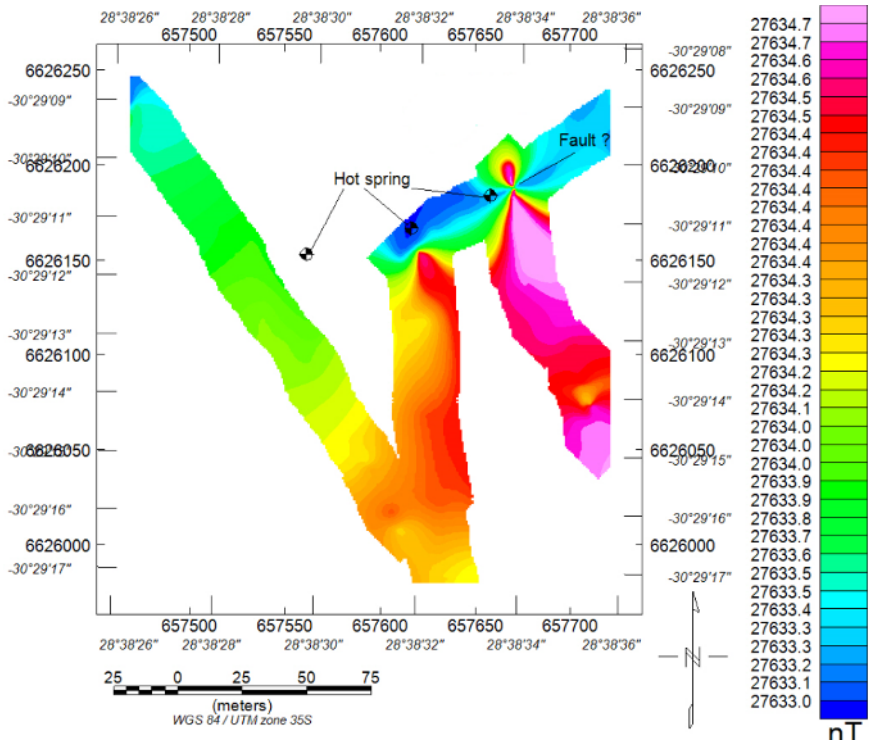

Fig. 4. Magnetic map produced at a grid cell size of 1 m.

Table 1

Sample of magnetic readings at Polile Tshisa

X [°]	*Y* [°]	GPS_height [m]	Reading_1 [nT]	Diurnal_1 [nT]	Corrected [nT]	Time	Date
28.64212	–30.4866	1360.789	27616.876	–16.424	27633.3	13:49:59.80	05/29/12
28.64212	–30.4866	1360.735	27623.534	–9.766	27633.3	13:49:59.60	05/29/12
28.64212	–30.4866	1360.681	27623.96	–9.340	27633.3	13:49:59.40	05/29/12
28.64212	–30.4866	1360.628	27621.513	–11.787	27633.3	13:49:59.20	05/29/12
28.64212	–30.4866	1360.574	27618.573	–14.727	27633.3	13:49:59.00	05/29/12
28.64212	–30.4866	1360.54	27621.324	–11.976	27633.3	13:49:58.80	05/29/12
28.64212	–30.4866	1360.527	27624.978	–8.322	27633.3	13:49:58.60	05/29/12
28.64213	–30.4866	1360.514	27632.037	–1.263	27633.3	13:49:58.40	05/29/12
28.64213	–30.4866	1360.501	27635.632	2.332	27633.3	13:49:58.20	05/29/12
28.64213	–30.4866	1360.488	27633.31	0.010	27633.3	13:49:58.00	05/29/12
28.64213	–30.4866	1360.470	27630.625	–2.675	27633.3	13:49:57.80	05/29/12
28.64214	–30.4866	1360.449	27632.072	–1.228	27633.3	13:49:57.60	05/29/12
28.64214	–30.4865	1360.428	27634.68	1.380	27633.3	13:49:57.40	05/29/12
28.64214	–30.4865	1360.406	27638.985	5.685	27633.3	13:49:57.20	05/29/12
28.64214	–30.4865	1360.385	27640.587	7.287	27633.3	13:49:57.00	05/29/12
28.64214	–30.4865	1360.354	27637.336	4.036	27633.3	13:49:56.80	05/29/12
28.64215	–30.4865	1360.315	27634.981	1.681	27633.3	13:49:56.60	05/29/12
28.64215	–30.4865	1360.276	27634.591	1.291	27633.3	13:49:56.40	05/29/12
28.64215	–30.4865	1360.238	27635.551	2.251	27633.3	13:49:56.20	05/29/12
28.64215	–30.4865	1360.199	27638.56	5.260	27633.3	13:49:56.00	05/29/12
28.64215	–30.4865	1360.166	27640.662	7.362	27633.3	13:49:55.80	05/29/12
28.64216	–30.4865	1360.141	27636.606	3.306	27633.3	13:49:55.60	05/29/12
28.64216	–30.4865	1360.115	27633.287	–0.013	27633.3	13:49:55.40	05/29/12
28.64216	–30.4865	1360.089	27632.014	–1.286	27633.3	13:49:55.20	05/29/12
28.64216	–30.4865	1360.064	27634.284	0.984	27633.3	13:49:55.00	05/29/12
28.64216	–30.4865	1360.036	27637.53	4.230	27633.3	13:49:54.80	05/29/12
28.64217	–30.4865	1360.007	27642.044	8.744	27633.3	13:49:54.60	05/29/12
28.64217	–30.4865	1359.978	27639.692	6.392	27633.3	13:49:54.40	05/29/12
28.64217	–30.4865	1359.949	27636.889	3.589	27633.3	13:49:54.20	05/29/12
28.64217	–30.4865	1359.920	27636.167	2.867	27633.3	13:49:54.00	05/29/12
28.64217	–30.4865	1359.892	27639.147	5.847	27633.3	13:49:53.80	05/29/12
28.64218	–30.4865	1359.867	27643.981	10.681	27633.3	13:49:53.60	05/29/12
28.64218	–30.4865	1359.842	27649.235	15.935	27633.3	13:49:53.40	05/29/12
28.64218	–30.4865	1359.816	27648.192	14.892	27633.3	13:49:53.20	05/29/12
28.64218	–30.4865	1359.791	27647.845	14.545	27633.3	13:49:53.00	05/29/12
28.64218	–30.4865	1359.774	27651.505	18.205	27633.3	13:49:52.80	05/29/12

to be continued

Table 1 (continuation)

X [°]	Y [°]	GPS_height [m]	Reading_1 [nT]	Diurnal 1 [nT]	Corrected [nT]	Time	Date
28.64219	–30.4865	1359.767	27656.119	22.819	27633.3	13:49:52.60	05/29/12
28.64219	–30.4865	1359.760	27662.603	29.303	27633.3	13:49:52.40	05/29/12
28.64219	–30.4865	1359.752	27668.121	34.821	27633.3	13:49:52.20	05/29/12
28.64219	–30.4865	1359.745	27667.763	34.463	27633.3	13:49:52.00	05/29/12
28.6422	–30.4865	1359.739	27668.977	35.677	27633.3	13:49:51.80	05/29/12
28.6422	–30.4865	1359.734	27676.68	43.380	27633.3	13:49:51.60	05/29/12
28.6422	–30.4865	1359.729	27680.699	47.399	27633.3	13:49:51.40	05/29/12
28.6422	–30.4865	1359.724	27688.957	55.657	27633.3	13:49:51.20	05/29/12
28.6422	–30.4865	1359.719	27691.569	58.269	27633.3	13:49:51.00	05/29/12
28.64221	–30.4865	1359.717	27690.99	57.690	27633.3	13:49:50.80	05/29/12
28.64221	–30.4865	1359.716	27694.13	60.830	27633.3	13:49:50.60	05/29/12
28.64221	–30.4865	1359.716	27698.642	65.342	27633.3	13:49:50.40	05/29/12
28.64221	–30.4865	1359.716	27703.999	70.699	27633.3	13:49:50.20	05/29/12
28.64222	–30.4865	1359.715	27709.518	76.218	27633.3	13:49:50.00	05/29/12
28.64222	–30.4865	1359.727	27709.386	76.086	27633.3	13:49:49.80	05/29/12
28.64222	–30.4865	1359.751	27713.465	80.165	27633.3	13:49:49.60	05/29/12
28.64222	–30.4865	1359.775	27722.623	89.323	27633.3	13:49:49.40	05/29/12
28.64223	–30.4865	1359.799	27727.628	94.328	27633.3	13:49:49.20	05/29/12
28.64223	–30.4865	1359.823	27737.051	103.751	27633.3	13:49:49.00	05/29/12
28.64223	–30.4865	1359.837	27740.421	107.121	27633.3	13:49:48.80	05/29/12
28.64223	–30.4865	1359.842	27741.883	108.583	27633.3	13:49:48.60	05/29/12
28.64223	–30.4865	1359.847	27746.097	112.797	27633.3	13:49:48.40	05/29/12
28.64223	–30.4865	1359.851	27749.984	116.684	27633.3	13:49:48.20	05/29/12
28.64224	–30.4865	1359.856	27751.505	118.205	27633.3	13:49:48.00	05/29/12
28.64224	–30.4865	1359.855	27760.037	126.737	27633.3	13:49:47.80	05/29/12
28.64224	–30.4865	1359.850	27765.333	132.033	27633.3	13:49:47.60	05/29/12
28.64224	–30.4865	1359.844	27767.607	134.307	27633.3	13:49:47.40	05/29/12
28.64224	–30.4865	1359.838	27771.036	137.736	27633.3	13:49:47.20	05/29/12
28.64224	–30.4865	1359.833	27778.494	145.194	27633.3	13:49:47.00	05/29/12
28.64225	–30.4865	1359.830	27785.487	152.187	27633.3	13:49:46.80	05/29/12
28.64225	–30.4865	1359.830	27792.654	159.354	27633.3	13:49:46.60	05/29/12
28.64225	–30.4865	1359.830	27804.345	171.045	27633.3	13:49:46.40	05/29/12
28.64225	–30.4865	1359.831	27808.339	175.039	27633.3	13:49:46.20	05/29/12
28.64225	–30.4865	1359.831	27811.176	177.876	27633.3	13:49:46.00	05/29/12
28.64225	–30.4865	1359.831	27817.256	183.956	27633.3	13:49:45.80	05/29/12
28.64225	–30.4865	1359.831	27826.289	192.989	27633.3	13:49:45.60	05/29/12

to be continued

Table 1 (continuation)

X [°]	*Y* [°]	GPS_height [m]	Reading_1 [nT]	Diurnal 1 [nT]	Corrected [nT]	Time	Date
28.64226	–30.4865	1359.831	27831.112	197.812	27633.3	13:49:45.40	05/29/12
28.64226	–30.4865	1359.830	27837.302	204.002	27633.3	13:49:45.20	05/29/12
28.64226	–30.4865	1359.830	27837.878	204.578	27633.3	13:49:45.00	05/29/12
28.64226	–30.4865	1359.825	27834.249	200.949	27633.3	13:49:44.80	05/29/12
28.64226	–30.4865	1359.816	27836.724	203.424	27633.3	13:49:44.60	05/29/12
28.64226	–30.4864	1359.807	27840.916	207.616	27633.3	13:49:44.40	05/29/12
28.64226	–30.4864	1359.798	27838.404	205.104	27633.3	13:49:44.20	05/29/12
28.64226	–30.4864	1359.789	27842.434	209.134	27633.3	13:49:44.00	05/29/12
28.64227	–30.4864	1359.790	27845.238	211.938	27633.3	13:49:43.80	05/29/12
28.64227	–30.4864	1359.802	27840.98	207.680	27633.3	13:49:43.60	05/29/12
28.64227	–30.4864	1359.815	27846.563	213.263	27633.3	13:49:43.40	05/29/12
28.64227	–30.4864	1359.827	27858.536	225.236	27633.3	13:49:43.20	05/29/12
28.64227	–30.4864	1359.839	27868.502	235.202	27633.3	13:49:43.00	05/29/12
28.64227	–30.4864	1359.834	27877.287	243.987	27633.3	13:49:42.80	05/29/12
28.64228	–30.4864	1359.813	27891.319	258.019	27633.3	13:49:42.60	05/29/12
28.64228	–30.4864	1359.792	27898.842	265.542	27633.3	13:49:42.40	05/29/12
28.64228	–30.4864	1359.770	27905.877	272.577	27633.3	13:49:42.20	05/29/12
28.64228	–30.4864	1359.749	27922.575	289.275	27633.3	13:49:42.00	05/29/12
28.64228	–30.4864	1359.727	27945.254	311.954	27633.3	13:49:41.80	05/29/12
28.64228	–30.4864	1359.706	27962.899	329.599	27633.3	13:49:41.60	05/29/12
28.64229	–30.4864	1359.685	27991.921	358.621	27633.3	13:49:41.40	05/29/12
28.64229	–30.4864	1359.664	28014.035	380.735	27633.3	13:49:41.20	05/29/12
28.64229	–30.4864	1359.643	28013.811	380.511	27633.3	13:49:41.00	05/29/12
28.64229	–30.4864	1359.611	28024.038	390.738	27633.3	13:49:40.80	05/29/12
28.6423	–30.4864	1359.569	28042.894	409.594	27633.3	13:49:40.60	05/29/12
28.6423	–30.4864	1359.527	28035.862	402.562	27633.3	13:49:40.40	05/29/12
28.6423	–30.4864	1359.485	28014.74	381.440	27633.3	13:49:40.20	05/29/12

mately 28 m. At this point it shows a slight decrease, but in general the profile remains constant up to 200 m. The increase in signal at the left side at approximately 28 m is possibly related to a fault resulting in the block to the right having moved up relative to the other block.

The second profile (Fig. 7) displays two peaks, one at 20 m, and the other 80.5 m. These peaks are possibly due to the presence of a wide dolerite dyke or two narrow dykes located directly beneath the peaks. A similar situation can be observed in Fig. 8; groundwater can be targeted besides these peaks related to the occurrence of dolerite dykes. Dolerites always cause a

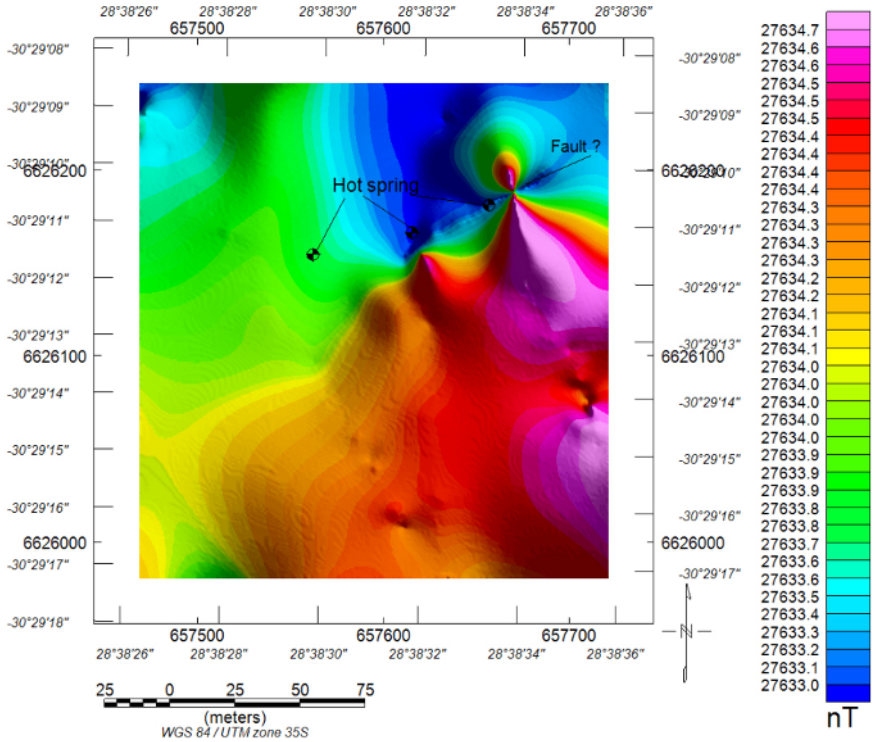

Fig. 5. Magnetic map derived from Fig. 3 but at a grid cell size of 14 m.

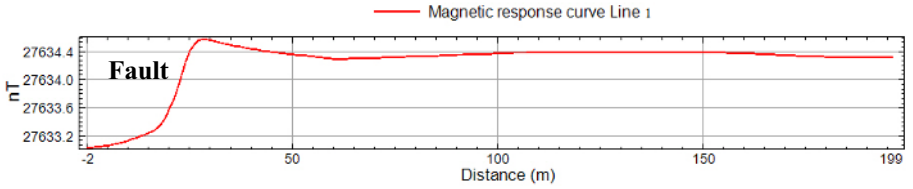

Fig. 6. Polile Tshisa magnetic profile in a SE-NW direction.

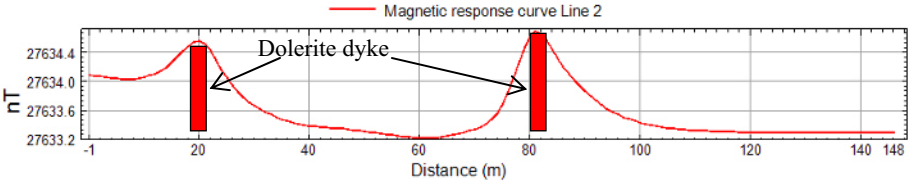

Fig. 7. Polile Tshisa magnetic profile in a SW-NE direction.

chilly margin to occur at the contact with the country rock. All the collected magnetic data can be seen in Table 1.

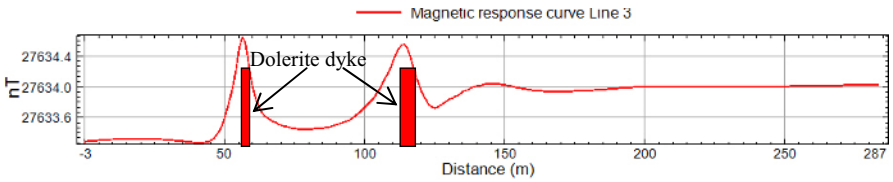

Fig. 8. Polile Tshisa second magnetic profile in a SW-NE direction.

3.3 Electromagnetic survey

The acquisition of data was organized for the survey along profiles oriented SE-NW (Lines 1 and 2, see Fig. 9). Profiles were set so in a quasi-perpendicular direction to the one of the structure that hosts the hot springs that wells up at three different places. Another profile, NE-SW (Line 3, see Fig. 9) was also set for a generalized coverage of the area, a better visualization and interpretation.

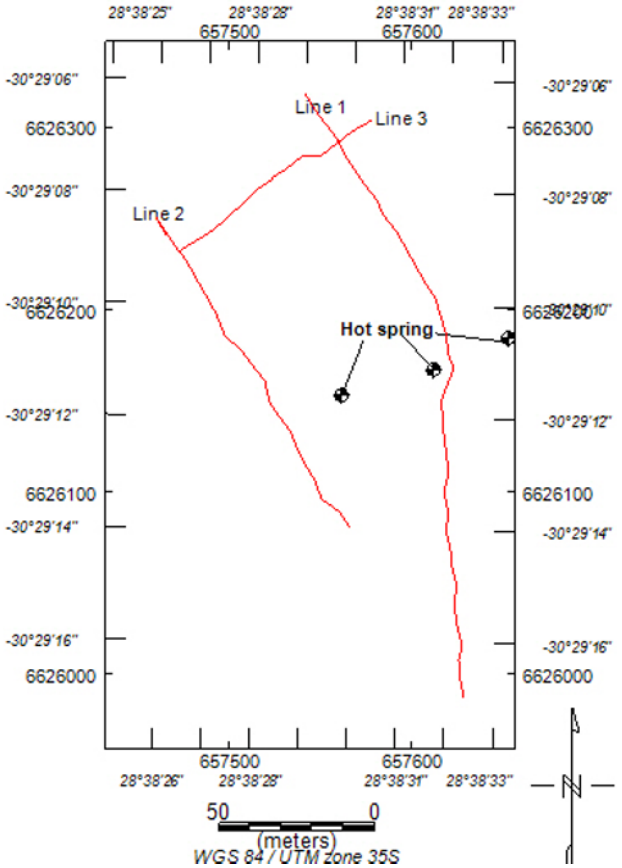

Fig. 9. Lines in red were set for data acquisition using the vertical and horizontal dipoles at intercoil spacing of 20 m at the Polile Tshisa hot spring.

Three lines (Lines 1, 2, and 3, Fig. 9) of combined vertical and horizontal dipole mode were set and data were acquired using an intercoil spacing of 20 m (SE-NW) profiles for Lines 1 and 2, and a third line (Line 3) in an NE-SW profile was set with an intercoil spacing of 20 m. The station spacing was 10 m. For the first line, with 20 m as intercoil spacing (Fig. 10), it was observed that between 0 and 50 m, 70 and 130 m, and from 220 to almost 270 m, the horizontal dipole is higher than the vertical dipole, which is indicative of a conductance that decreases with depth. It is also indicative of a shallow regolith.

Two contrasting anomalies can be seen around 170 m; the vertical dipole showing a positive peak might be indicative of a weathered and fractured zone, and the horizontal dipole showing a low peak at the same place can be

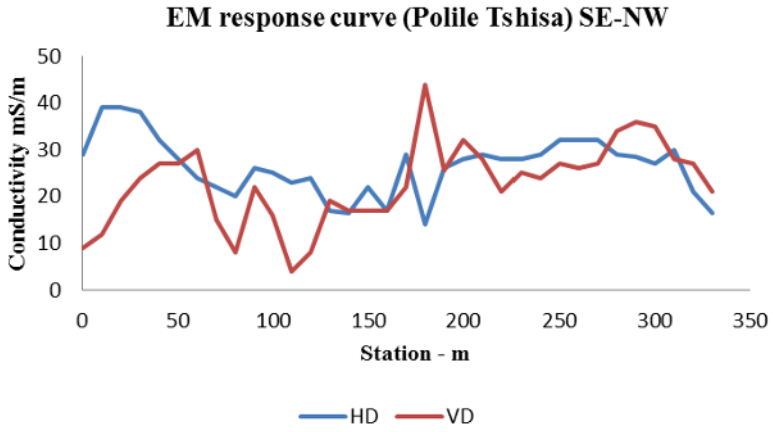

Fig. 10. Line 1 oriented SE-NW (intercoil spacing: 20 m).

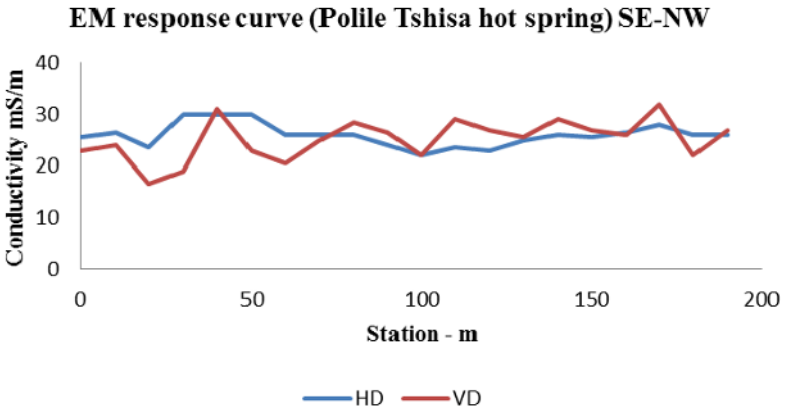

Fig. 11. Line 2 (intercoil spacing: 20 m).

Table 2

Polile Tshisa hot spring L1_20, horizontal and vertical dipole

Sta [m]	*HD* [mS/m]	*VD* [mS/m]	*X* [m]	*Y* [m]	*Z* [m]	Direction SE-NW
0	29	9	657629	6625987	1355	SE
10	39	12	657627	6625996	1355	
20	39	19	657626	6626008	1356	
30	38	24	657628	6626016	1357	
40	32	27	657625	6626027	1349	
50	28	27	657623	6626039	1350	
60	24	30	657625	6626048	1350	
70	22	15	657622	6626059	1349	
80	20	8	657621	6626069	1349	
90	26	22	657619	6626080	1351	
100	25	16	657620	6626087	1352	
110	23	4	657618	6626101	1354	
120	24	8	657620	6626110	1355	
130	17	19	657619	6626121	1357	
140	16.5	17	657618	6626132	1358	
150	22	17	657618	6626141	1359	
160	17	17	657616	6626148	1360	
170	29	22	657619	6626157	1360	
180	14	44	657623	6626168	1361	
190	26	25.5	657620	6626175	1361	
200	28	32	657619	6626188	1363	
210	29	28	657613	6626206	1365	
220	28	21	657607	6626216	1366	
230	28	25	657602	6626224	1367	
240	29	24	657598	6626233	1368	
250	32	27	657592	6626243	1369	
260	32	26	657585	6626252	1370	
270	32	27	657581	6626260	1370	
280	29	34	657575	6626268	1371	
290	28.5	36	657569	6626277	1372	
300	27	35	657564	6626285	1372	
310	30	28	657559	6626294	1373	
320	21	27	657547	6626310	1374	
330	16.5	21	657542	6626319	1376	NW

interpreted as a vertical dyke. Dykes in the Karoo aquifers are good indicators for groundwater exploration. This area may have two structures favourable for groundwater. Between 60 and 130 m, the vertical dipole displays two remarkable lows separated by a high. The two peaks can be related to dolerite dykes with a fracture in between them. Thus the potential of finding a productive well is high in this area. There is a quite good variation in conductivity for the horizontal dipole (~40 to 13 mS/m), whilst for the vertical dipole the variation is a bit high (9 to 44 mS/m). The complete set of data is presented in Table 2.

For Line 2, with 20 m as intercoil spacing (Fig. 11), there is no remarkable variation in the conductivity for the horizontal dipole (26-30 mS/m). This may signify that there is no much variation either in mineralogy or porosity. The vertical dipole has higher variation (16.5-32 mS/m) than the horizontal dipole. It is quite clear that between 0 and 40 m and between 42 and 70 m the response of the horizontal dipole is higher than that of the vertical one. This is indicative of a shallow regolith, as observed for the previous profiles. Between 0 and 30 m, both the horizontal and vertical dipole signatures almost dovetail. The set of data is reprised in Table 3.

For Line 3 (Table 4), with intercoil spacing of 20 m (Fig. 12), the vertical dipole response seems higher than that of the horizontal dipole from 0 to 70 m. The signatures of the dipoles (horizontal HD and vertical VD) almost dovetail between 15 and 36 m. On this profile the survey may have intersected a dyke. It may imply that there is a change in the physical properties of the rocks because of the similar responses for the vertical and the horizontal dipoles.

As for Line 2 in Fig. 10 (20 m intercoil spacing), there is similarity in horizontal dipole patterns. It can be seen that from 50 to 110 m, the profile is almost flat like in Fig. 10, and not showing considerable variations.

The vertical dipole shows high conductivities at two points, at 40 and 60 m (> 40 mS/m), with lower conductivities of 18.5 and 24.5 mS/m at 30 and 80 m. These high conductivities from the vertical dipole indicate a possible fault or fracture below the surface. The complete set of data can be seen in Table 4.

The depth-conductivity model (Fig. 13) from Line 1 data at the Polile Tshisa hot spring shows two high conductivity zones (*e.g.*, ≥ 30 mS/m) at the southeastern end of the profile and from about 175 m to the northern end of the profile. Both zones of high conductivity extend from surface to about 8 m depth.

The high conductivity zones can be interpreted as highly weathered sandstones. The area of the Polile Tshisa hot spring was observed to have sandstones that are weathered, leaving loosed particles of sand and whitish kaolinised material. The dashed lines marked in Fig. 12 are inferred to be

Table 3

Polile Tshisa hot spring line 2: L2-20, horizontal and vertical dipole

Sta [m]	X_Dist	*HD* [mS/m]	*VD* [mS/m]	*X* [m]	*Y* [m]	*Z* [m]	Direction N-S
190	0	26	27	657566	6626081	1359	SE
180	10	26	22	657561	6626089	1360	
170	20	28	32	657551	6626096	1361	
160	30	26.5	26	657547	6626106	1362	
150	40	25.5	27	657542	6626115	1364	
140	50	26	29	657538	6626123	1366	
130	60	25	25.5	657533	6626134	1367	
120	70	23	27	657533	6626134	1367	
110	80	23.5	29	657528	6626141	1367	
100	90	22	22	657522	6626149	1370	
90	100	24	26.5	657520	6626161	1371	
80	110	26	28.5	657520	6626161	1370	
70	120	26	25	657512	6626170	1371	
60	130	26	20.5	657507	6626178	1371	
50	140	30	23	657498	6626186	1372	
40	150	30	31	657493	6626198	1373	
30	160	30	19	657477	6626227	1375	
20	170	23.5	16.5	657470	6626235	1376	
10	180	26.5	24	657460	6626251	1378	
0	190	25.5	23	657466	6626241	1377	NW

Table 4

Polile Tshisa line 3: L3_20, horizontal and vertical dipole

Sta [m]	X_Dist	*HD* [mS/m]	*VD* [mS/m]	*X* [m]	*Y* [m]	*Z* [m]	Direction
110	0	32	34	657472	6626232	1377	NE
100	10	40	36	657491	6626244	1376	
90	20	39	40	657499	6626250	1376	
80	30	38	24.5	657509	6626259	1376	
70	40	38	36	657515	6626266	1377	
60	50	36	47	657524	6626272	1376	
50	60	34	34	657524	6626273	1376	
40	70	40	47	657531	6626277	1374	
30	80	25.5	18.5	657540	6626284	1374	
20	90	15	20	657551	6626285	1374	
10	100	35	42	657567	6626298	1372	
0	110	36	42	657578	6626304	1373	NW

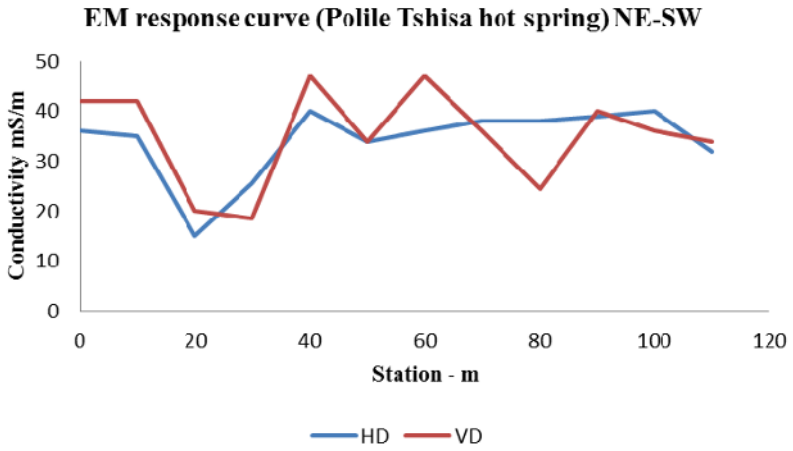

Fig. 12. Line 3 (intercoil spacing: 20).

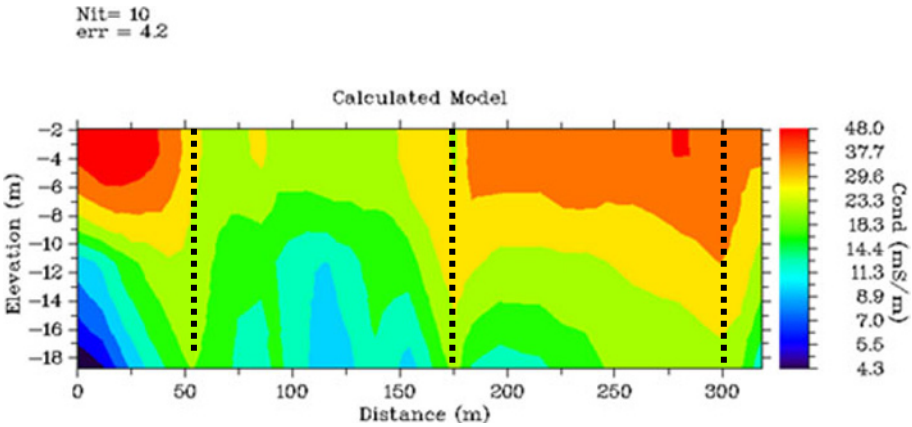

Fig. 13. Polile Tshisa hot spring conductivity-depth model. The dotted lines mark positions of inferred faults. Nit is the number of iterations, and err is the least squares error between calculated and observed conductivities.

either large faults or fractures along which water can migrate upwards easily. Generally, it transpires from the depth modelling that the conductivity is decreasing with depth for the maximum investigated depth (≈ 20 m).

3.4 Hydrogeological conceptual model of the Polile Tshisa hot spring area

The hydrogeological conceptual model (Fig. 14) shows that the area of the Polile Tshisa hot spring is structurally controlled by faults and fractures with the intrusion of dolerites. This is indicative of a potential target for high yield aquifers. Fractures and faults are conduits for groundwater flow. The

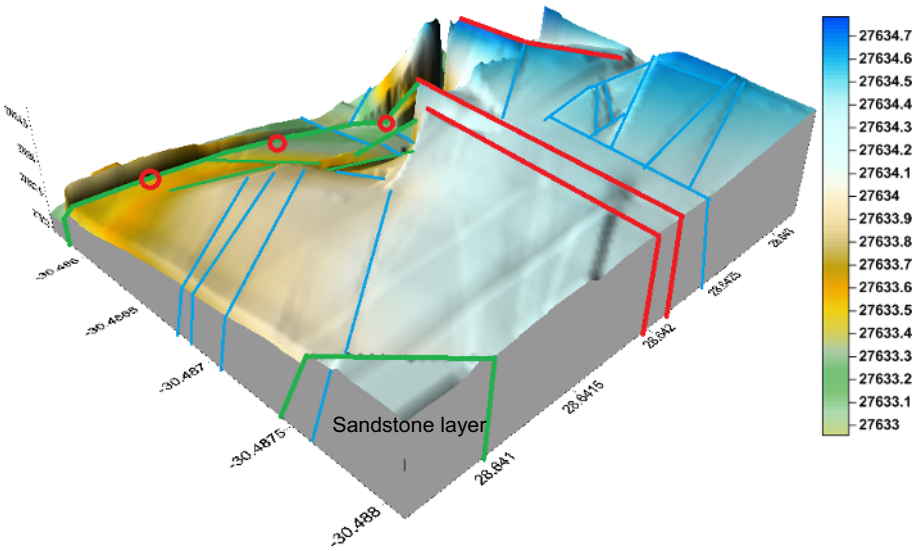

Fig. 14. Hydrogeological conceptual model of the Polile Tshisa hot spring area. Faults are in green, fractures in blue, and dolerites in red. The grey surface represents the sandstone layer.

coarse-grain sandstone of this area is a preferred lithology on the hydrogeological point of view. It is well known that the coarser the grain, the higher the porosity, and the finer the grains, the lower the porosity. The WSW-ENE trending fault, as seen in Fig. 8, along which the water from the three hot springs wells up is very remarkable in this conceptual model. Two dolerite dykes seen in Figs. 6 and 7, oriented N-S, have high magnetic values and are parallel (Fig. 14). It is quite clear that extensional faulting (σ_1 vertical, σ_2, and σ_3 horizontal) prevailed where the magnetic values are low, as can be seen at the north side in Fig. 8.

4. DISCUSSION AND CONCLUSIONS

The neotectonics belt near the country of Lesotho is also known for the occurrence of many hot springs, which are indicative of circulation of groundwater at great depths; the occurrence of these springs indicates that they are connected by a major neotectonic fault that stretches from west (Aliwal North) to east (Polile Tshisa). The flooding that occurred in an abnormally well-developed fissure zone, through which a lot of water gushed out during the construction of the Orange–Fish tunnel (Olivier 1972), is a proof that neotectonics is at work in the northern neotectonics belt. Whittingan (1970) noted that the flow of the thermal spring at Badfontein increased markedly

for a period of at least three months after a local earthquake. The Karoo rocks were intruded by dolerite dykes and sills. Strongest magnetic values at the Polile Tshisa hot springs indicate the presence of dolerite dykes or sills, or even unweathered solid geological basement (*e.g.*, Street *et al.* 2002). At Polile Tshisa the magnetic profile in Fig. 6 is typical of a fault that has moved two blocks with a dip-slip component. The water at Polile Tshisa wells up at three different places, which are connected by a fault (Fig. 14) that has possibly cut across the dolerite dykes. Electromagnetic profiles in all the three hot springs are indicative of faults or fractures at some places and dolerite dykes at others. These profiles also show that the weathering process is underway. At Polile Tshisa combined profiles of both horizontal and vertical dipole show that the horizontal dipole is higher than the vertical one at some places; this is always an indication for a shallow regolith (*e.g.*, Barry *et al.* 2010).

The hot springs in the Eastern Cape northern neotectonic belt are connected or occur along an east-west neotectonic fault that is a regional structure. The magnetic and electromagnetic data have helped to identify fractured or faulted zones with different degrees of weathering. At some places one can mention the presence of dolerite dykes, known for their potential to localise groundwater in the Karoo. It is clear that the three places from where the water of the Polile Tshisa hot spring wells up are connected by a WSW-ENE trending fault. The well located near the dolerite dykes, as seen in Fig. 14, is a great target to drill for a productive borehole because dolerite dykes are localisers of groundwater. The combination of seismic activity in the Kokstad–Koffiefontein seismic belt, the occurrence of hot springs in that belt, and the interpreted derived fauts, fractures and dolerite dykes, makes the Polile Tshisa area a potential environment to explore for groundwater.

Acknowledgements. The authors would like to thank the Govan Mbeki development Research Center (GMRDC) at Fort Hare University and the National Research Fund (NRF) of South Africa for financial assistance in this project. The Council of Geoscience of South Africa is greatly acknowledged for the logistical support.

References

Barry, B., B. Kortatsi, G. Forkuor, M.K. Gumma, R. Namara, L.-M. Rebelo, J. van den Berg, and W. Laube (2010), Shallow groundwater in the Atankwidi Catchment of the White Volta Basin: Current status and future sustainabil-

ity, Res. Rep. 139, International Water Management Institute (IWMI), Colombo, Sri Lanka, 30 pp., DOI: 10.5337/2010.234.

Delvaux, D.F., and M. Hanon (1993), Neotectonics of the Mbeya Area, SW Tanzania, *Mus. Roy. Afr. Centr. Dept. Geol. Min. Rapp. Ann*. **1991-1992**, 87-97.

Hartnady, C.J.H. (1985), Uplift, faulting seismicity, thermal spring and possible incipient volcanic activity in the Lesotho–Natal region, SE Africa: The Quathlamba hotspot hypothesis, *Tectonics* **4**, 4, 371-377, DOI: 10.1029/TC004i004p00371.

Kent, L.E. (1969), The thermal waters in the Republic of South Africa. **In:** *Proc. 23rd Int. Geol. Cong. "Mineral and Thermal Waters of the World", Czechoslovakia 1968*, Vol. 19, 143-164.

Maud, R.R., T.C. Partridge, and J.N. Dunlevey (1998), The Lesotho "volcanic" event of February 1983, *South Afr. J. Geol.* **101**, 4, 313-322.

Meissner, R., and T. Wever (1986), Intracontinental seismicity, strength of crustal units, and the seismic signature of fault zones, *Philos. Trans. Roy. Soc. Lond. A* **317**, 1539, 45-61, DOI: 10.1098/rsta.1986.0024.

Olivier, H.J. (1972), Geohydrological investigation of the flooding at shaft 2, Orange–Fish tunnel, north-eastern Cape Province, *Trans. Geol. Soc. South Afr.* **75**, 197-224.

Olivier, J., J.S. Venter, and C.Z. Jonker (2011), Thermal and chemical characteristics of hot water springs in the northern part of the Limpopo Province, South Africa, *Water SA* **37**, 4, 427-436, DOI: 10.4314/wsa.v37i4.1.

Spurr, A.M.M. (1953), The geology of the Songwe river, Mbeya district, Report AMMS/17, Geological Survey of Tanganyika (unpublished).

Street, G.J., G. Pracilio, and A.M. Anderson-Mayes (2002), Interpretation of geophysical data for salt hazard identification and catchment management in Southwest Western Australia, *Explor. Geophys.* **33**, 2, 65-72, DOI: 10.1071/EG02065.

Wittingham, J.K. (1970), Report of geophysical investigations along the route of the Orange–Fish tunnel, Cape Province, Geol. Surv. South Africa (unpublished).

Received 20 January 2015
Received in revised form 18 April 2015
Accepted 23 June 2015